RARE B DECAYS TO CHARMLESS MESONS

B.H. BEHRENS
Department of Physics, University of Colorado,
Boulder, Colorado 80309, USA

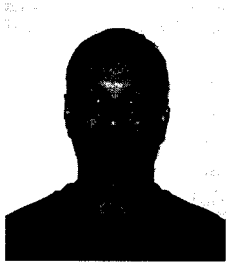

We have searched for two-body charmless hadronic decays of the B meson. In a data sample of 3.3 million $B\bar{B}$ pairs collected with the CLEO II detector, we observe five signals with greater than 3σ significance: $B^0 \to K^+\pi^-$,$B^+ \to K^0\pi^+$,$B^+ \to \eta' K^+$, $B^0 \to \eta' K^0$, and $B^+ \to \omega K^+$. We also see some evidence for the decay $B \to \phi K^*$, and set upper limits for many other decay modes.

1 Does the Standard Model explain CP violation?

In the Standard Model, transitions between quark flavors are described by the CKM matrix[1,2]. Assuming the CKM matrix is unitary and complex, the nine matrix elements depend on four parameters. Wolfenstein[3] parameterized the CKM matrix this way:

$$\begin{pmatrix} V_{ud} & V_{us} & V_{ub} \\ V_{cd} & V_{cs} & V_{cb} \\ V_{td} & V_{ts} & V_{tb} \end{pmatrix} \to \begin{pmatrix} 1-\frac{\lambda^2}{2} & \lambda & A\lambda^3(\rho-i\eta) \\ -\lambda & 1-\frac{\lambda^2}{2} & A\lambda^2 \\ A\lambda^3(1-\rho-i\eta) & -A\lambda^2 & 1 \end{pmatrix}$$

CP violation occurs because of the complex number $\rho - i\eta$ in the CKM matrix.

If the CKM matrix is unitary then the parameters ρ and η can be thought of as coordinates defining the apex of a triangle as shown in figure 1. By measuring the angles, α, β, and γ, of the unitarity triangle, and the lengths of each of the sides, we can greatly increase our understanding of CP violation. Physics beyond the Standard Model could result in inconsistencies between the various measurements[4,5]. In the future, charmless hadronic decays of B mesons will provide valuable information about the angles of the unitarity triangle. For example, γ can be measured in $B \to K\pi$ decays, α can be measured with $B \to \pi\pi$ decays, and β can be measured in $B \to \eta' K^0$ decays[5].

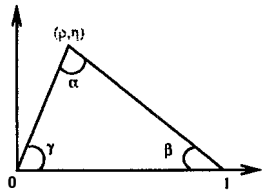

Figure 1: The unitarity triangle.

2 Data Sample and Analysis

The data set used in this analysis was collected with the CLEO II detector [6] at the Cornell Electron Storage Ring (CESR). All CLEO II data taken on the $\Upsilon(4S)$ resonance were used in this analysis. The total integrated luminosity was 3.11 fb^{-1} of on-resonance and 1.61 fb^{-1} of off-resonance data (used to determine background PDFs), corresponding to 3.3 million $B\bar{B}$ events.

The primary observable in this analysis is M, the beam constrained B mass. Each B meson must have energy equal to the energy of one beam, E_{beam}. Since we know the beam energy with higher accuracy than we can measure the energy of the B meson, we calculate the B mass assuming its energy is equal to E_{beam}. The beam constrained mass has a typical resolution of 3 MeV. Another important quantity, ΔE, measures the difference between the measured B energy (E_B) and E_{beam} ($\Delta E = E_B - E_{\text{beam}}$). The resolution in ΔE is typically about 30 MeV. Continuum background is reduced by requiring the cosine of the angle between the thrust axis of the B meson candidate and the thrust axis of the rest of the event to be less than 0.9. Continuum events tend to be "jetty" so the thrust axis of the B candidate is nearly aligned with the thrust axis of the rest of the event. Real B decays tend to have a more isotropic distribution of particles.

Loose cuts are applied to M, ΔE, event shape, daughter masses, dE/dx, and helicity (depending on the specific mode). Events passing these consistency cuts are then analyzed with a maximum likelihood fit. The results of the fits are shown below. This paper summarizes three recent CLEO publications [7,8,9]. Please see those publications for further details of the analysis and likelihood fit method.

3 Results

3.1 $B \to K\pi$

The results of the maximum likelihood fits for B decay modes involving poins and kaons are shown in figure 2. We observe three signals, $Br(B^0 \to K^+\pi^-) = 1.5^{+0.5}_{-0.4} \pm 0.1 \pm 0.1 \times 10^{-5}$, $Br(B^+ \to K^0\pi^+) = 2.3^{+1.1}_{-1.0} \pm 0.3 \pm 0.2 \times 10^{-5}$, and $Br(B^+ \to h^+\pi^0) = 1.6^{+0.6}_{-0.5} \pm 0.3 \pm 0.2 \times 10^{-5}$ (h denotes either a kaon or a pion) with 5.6, 3.2, and 5.5σ significance, respectively (here and throughout the paper charge conjugate modes are implied). Figure 3 shows plots of M and ΔE for the three modes with signals. Note that the data shown in figure 3 and in subsequent M plots are a subset of the data that were included in the likelihood fit. Table 1 shows the experimental results and theoretical predictions for all combinations of kaons and pions studied.

3.2 $B \to \eta' K$

Our search for B decay modes involving η and η' mesons resulted in two observations: $Br(B^+ \to \eta' K^+) = 6.5^{+1.5}_{-1.4} \pm 0.9 \times 10^{-5}$ and $Br(B^0 \to \eta' K^0) = 4.7^{+2.7}_{-2.0} \pm 0.9 \times 10^{-5}$. Figure 4 shows

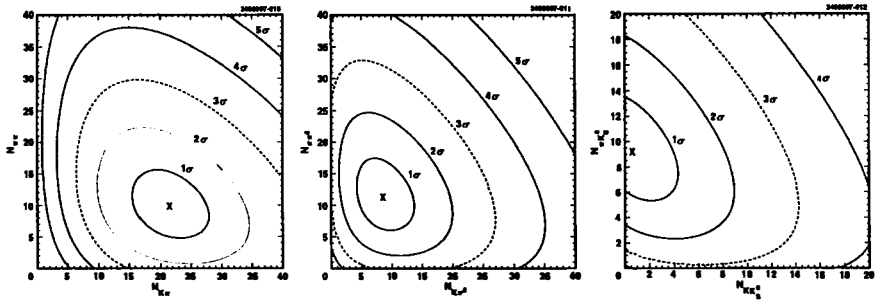

Figure 2: Contour of $-2ln(\mathcal{L})$ for a charged track and either a $\pi^{\pm}$ (left), a π^0 (center) or a K^0 (right), given by the likelihood fit. The vertical axes are the number of events in which the charged track is consistent with a $\pi^{\pm}$, while the horizontal axes are the number of events in which the charged track is consistent with a $K^{\pm}$.

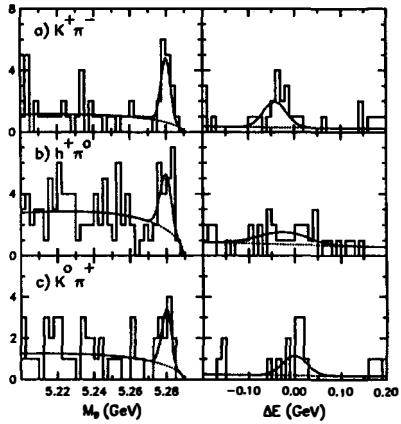

Figure 3: M and ΔE plots for (a) $B^0 \to K^+\pi^-$, (b) $B^+ \to h^+\pi^0$, and (c) $B^+ \to K^0\pi^+$. The scaled projection of the total likelihood fit (solid curve) and the continuum background component (dotted curve) are overlaid.

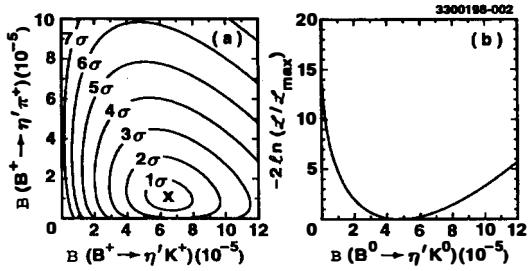

Figure 4: Maximum likelihood fit results (a) $-2ln(\mathcal{L})$ contours of the branching ratio of $B^{\pm} \to \eta' h^{\pm}$ where $h^{\pm}$ is a $\pi^{\pm}$ (vertical axis) or $K^{\pm}$ (horizontal axis) and (b) $-2ln(\mathcal{L})$ as a function of the branching ratio of $B^0 \to \eta' K^0$.

Table 1: Experimental results and theoretical predictions for decay modes involving kaons and pions.

Decay mode	$\mathcal{B}(10^{-5})$	Theory $\mathcal{B}$ (10^{-5})	References
$\pi^+\pi^-$	< 1.5	0.8–2.6	10– 19
$\pi^+\pi^0$	< 2.0	0.4–2.0	10– 19
$\pi^0\pi^0$	< 0.93	0.006–0.1	10– 19
$K^+\pi^-$	$1.5^{+0.5}_{-0.4} \pm 0.1 \pm 0.1$	0.7–2.4	10– 19
$K^+\pi^0$	< 1.6	0.3–1.3	10– 19
$K^0\pi^+$	$2.3^{+1.1}_{-1.0} \pm 0.3 \pm 0.2$	0.8–1.5	10– 19
$K^0\pi^0$	< 4.1	0.3–0.8	10– 19
K^+K^-	< 0.43	–	–
$K^+\bar{K}^0$	< 2.1	0.07–0.13	10– 19
$K^0\bar{K}^0$	< 1.7	0.07–0.12	10– 19
$h^+\pi^0$	$1.6^{+0.6}_{-0.5} \pm 0.3 \pm 0.2$	–	–

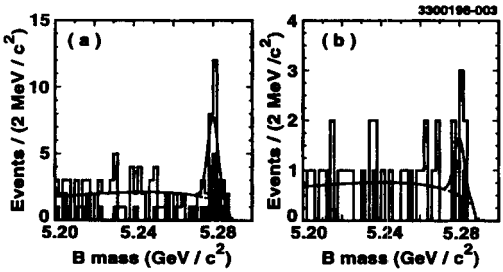

Figure 5: Constrained B mass (M) for (a) $B^+ \to \eta' K^+$, and (b) $B^0 \to \eta' K^0$. The scaled projection of the total likelihood fit (solid curve) and the continuum background component (dotted curve) are overlaid.

Table 2: Experimental results and theoretical predictions for decay modes involving η and η' mesons.

Decay mode	$\mathcal{B}(10^{-5})$	Theory $\mathcal{B}$ (10^{-5})	References
$B^+ \to \eta' K^+$	$6.5^{+1.5}_{-1.4} \pm 0.9$	$1.0 - 4.1$	11,20
$B^0 \to \eta' K^0$	$4.7^{+2.7}_{-2.0} \pm 0.9$	$0.9 - 3.3$	11,20
$B^+ \to \eta' \pi^+$	< 3.1	$0.8 - 1.7$	11,20
$B^0 \to \eta' \pi^0$	< 1.1	$0.4 - 1.4$	11,20
$B^0 \to \eta' \eta'$	< 4.7	$0.1 - 2.8$	11,20
$B^0 \to \eta' \eta$	< 2.7	$0.4 - 4.4$	11,20
$B^+ \to \eta' K^{*+}$	$< 13.$	$0.1 - 0.9$	11,20
$B^0 \to \eta' K^{*0}$	< 3.9	$0.8 - 1.7$	11,20
$B^+ \to \eta' \rho^+$	< 4.7	$1.1 - 5.7$	11,20
$B^0 \to \eta' \rho^0$	< 2.3	$0.2 - 1.2$	11,20
$B^+ \to \eta K^+$	< 1.4	$0.1 - 0.5$	11,20
$B^0 \to \eta K^0$	< 3.3	$0.1 - 0.2$	11,13,20
$B^+ \to \eta \pi^+$	< 1.5	$0.4 - 0.6$	11,13,20
$B^0 \to \eta \pi^0$	< 0.8	$0.2 - 0.4$	11,20
$B^0 \to \eta \eta$	< 1.8	$0.1 - 1.4$	11,13,20
$B^+ \to \eta K^{*+}$	< 3.0	$0.1 - 1.3$	11,20
$B^0 \to \eta K^{*0}$	< 3.0	$0.1 - 0.5$	11,13,20
$B^+ \to \eta \rho^+$	< 3.2	$0.8 - 4.4$	11,13,20
$B^0 \to \eta \rho^0$	< 1.3	$0.1 - 0.8$	11,13,20

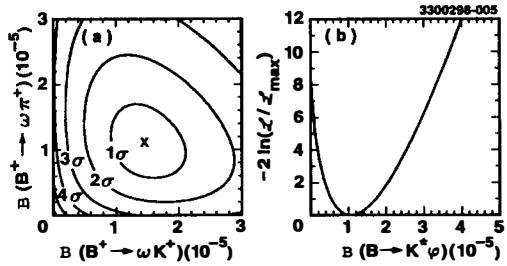

Figure 6: Maximum likelihood fit results (a) $-2ln(\mathcal{L})$ contours of the branching ratio of $B^+ \to \omega h^+$where $h^\pm$ is a $\pi^\pm$ (vertical axis) or $K^\pm$ (horizontal axis) and (b) $-2ln(\mathcal{L})$ as a function of the branching ratio of $B \to \phi K^*$.

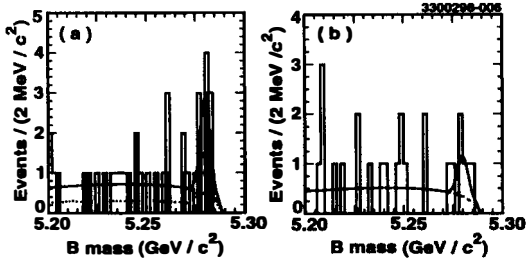

Figure 7: Constrained B mass (M) for (a) $B^+ \to \omega K^+$, and (b) ϕK^*. The scaled projection of the total likelihood fit (solid curve) and the continuum background component (dotted curve) are overlaid.

the likelihood functions ($-2ln(\mathcal{L})$) for the decays $B^+ \to \eta' K^+$ and $B^0 \to \eta' K^0$. Figure 5 shows the constrained B mass (M) for $B^+ \to \eta' K^+$ and $B^0 \to \eta' K^0$. Table 2 summarizes the experimental results and theoretical predictions for decay modes involving η and η' mesons. The observation of $B \to \eta' K$ decays with relatively large branching ratios inspired many new theoretical explanations [21]. Only more data will decide which explanation is correct.

3.3 $B^+ \to \omega K^+$ and $B \to \phi K^*$

We also searched for B decay modes involving ω and ϕ mesons. We observe a signal in the decay $B^+ \to \omega K^+$, with $Br(B^+ \to \omega K^+) = 1.5^{+0.7}_{-0.6} \pm 0.2 \times 10^{-5}$. We also see some evidence for the decay $B \to \phi K^*$ at the 2.9σ level. If we interpret this as a signal the branching ratio is $Br(B \to \phi K^*) = 1.1^{+0.6}_{-0.5} \pm 0.2 \times 10^{-5}$. Figure 6 shows the likelihood functions ($-2ln(\mathcal{L})$) for the decays $B^+ \to \omega K^+$ and $B \to \phi K^*$. Figure 7 shows the constrained B mass (M) for $B^+ \to \omega K^+$ and $B \to \phi K^*$. Table 3 summarizes the experimental results and theoretical predictions for decay modes involving ω and ϕ mesons.

References

1. N. Cabibbo, *Phys. Rev. Lett.* **10**, 531 (1963)
2. M. Kobayashi and T. Maskawa, *Prog. Theor. Phys.* **49** 652 (1973).
3. L. Wolfenstein, *Phys. Rev. Lett.* **51**, 1945 (1983).
4. See for example, M. Gronau and D. London, *Phys. Rev.* D **55**, 2845 (1997)

Table 3: Experimental results and theoretical predictions for decay modes involving ω and ϕ mesons.

Decay mode	$\mathcal{B}(10^{-5})$	Theory $\mathcal{B}$ (10^{-5})	References
$B^+ \to \omega K^+$	$1.5^{+0.7}_{-0.6} \pm 0.2$	$0.1 - 0.7$	11,13,17,20
$B^0 \to \omega K^0$	< 5.7	$0.1 - 0.4$	11,13,20
$B^+ \to \omega \pi^+$	< 2.3	$0.1 - 0.7$	11,13,17,20
$B^+ \to \omega h^+$	$2.5^{+0.8}_{-0.7} \pm 0.3$	–	–
$B^0 \to \omega \pi^0$	< 1.4	$0.1 - 1.2$	11,13,20
$B^0 \to \omega \eta'$	< 6.0	$0.3 - 1.7$	11,20
$B^0 \to \omega \eta$	< 1.2	$0.1 - 0.5$	11,20
$B^+ \to \omega K^{*+}$	< 8.7	$0.1 - 1.5$	11,13,16
$B^0 \to \omega K^{*0}$	< 2.3	$0.2 - 0.8$	11,13
$B^+ \to \omega \rho^+$	< 6.1	$1.1 - 2.5$	11,13,16
$B^0 \to \omega \rho^0$	< 1.1	0.04	11
$B^0 \to \omega \omega$	< 1.9	$0.1 - 0.3$	11,13
$B^+ \to \phi K^+$	< 0.5	$0.1 - 1.6$	10,11,13,14,15,17,20
$B^0 \to \phi K^0$	< 3.1	$0.1 - 1.3$	10,11,13,14,15,20
$B^+ \to \phi \pi^+$	< 0.5	$<< 0.1$	12,13,14,17,20
$B^0 \to \phi \pi^0$	< 0.5	$<< 0.1$	12,13,14,20
$B^0 \to \phi \eta'$	< 3.1	$<< 0.1$	12,20
$B^0 \to \phi \eta$	< 0.9	$<< 0.1$	12,13,20
$B^+ \to \phi K^{*+}$	< 4.1	$0.1 - 3.1$	10,11,13,15,16
$B^0 \to \phi K^{*0}$	< 2.1	$0.1 - 3.1$	10,11,13,15
$B^+ \to \phi \rho^+$	< 1.6	$<< 0.1$	12,13,16
$B^0 \to \phi \rho^0$	< 1.3	$<< 0.1$	12,13
$B^0 \to \phi \omega$	< 2.1	$<< 0.1$	12,13
$B^0 \to \phi \phi$	< 1.2	–	–

5. For an overview of interesting decay modes see J. L. Rosner, hep-ph/9801201, EFI-97-58.
6. Y. Kubota *et al.* (CLEO Collaboration), *Nucl. Instrum. Methods* A **320**, 66 (1992).
7. R. Godang *et al.* (CLEO Collaboration), *Phys. Rev. Lett.* **80**, 3456 (1998).
8. B. H. Behrens *et al.* (CLEO Collaboration), *Phys. Rev. Lett.* **80**, 3710 (1998).
9. T. Bergfeld *et al.* (CLEO Collaboration), CLNS 97-1537, submitted to Phys. Rev. Lett.
10. N.G. Deshpande and J. Trampetic, *Phys. Rev.* D **41**, 895 (1990).
11. L.-L. Chau *et al.*, *Phys. Rev.* D **43**, 2176 (1991).
12. D. Du and Z. Xing, *Phys. Lett.* B **312**, 199 (1993).
13. A. Deandrea, N. Di Bartolomeo, R. Gatto, G. Nardulli, *Phys. Lett.* B **318**, 549 (1993); A. Deandrea, N. Di Bartolomeo, R. Gatto, F. Feruglio, G. Nardulli, *Phys. Lett.* B **320**, 170 (1994).
14. R. Fleischer, *Z. Phys.* C **58**, 483 (1993).
15. A. J. Davies, T. Hayashi, M. Matsuda, and M. Tanimoto, *Phys. Rev.* D **49**, 5882 (1994).
16. G. Kramer, W. F. Palmer, and H. Simma, *Nucl. Phys.* B **428**, 429 (1994).
17. G. Kramer, W. F. Palmer, and H. Simma, *Z. Phys.* C **66**, 429 (1995).
18. G. Kramer and W. F. Palmer, *Phys. Rev.* D **52**, 6411 (1995).
19. D. Ebert, R. N. Faustov, and V. O. Galkin, *Phys. Rev.* D **56**, 312 (1997).
20. D. Du and L. Guo, *Z. Phys.* C **75**, 9 (1997).
21. A summary can be found in D. Atwood and A. Soni, hep-ph/9712243, Proceedings of the International Europhysics Conference on High Energy Physics, Jerusalem, Aug. 1997.